

Available online at [www.sciencedirect.com](http://www.sciencedirect.com)**ScienceDirect**

Procedia Engineering 108 (2015) 496 – 503

**Procedia  
Engineering**[www.elsevier.com/locate/procedia](http://www.elsevier.com/locate/procedia)

7th Scientific-Technical Conference Material Problems in Civil Engineering (MATBUD'2015)

## The stiffness and bearing capacity of Polymer Flexible Joint under shear load

Paweł Kisiel<sup>a,\*</sup><sup>a</sup>*Cracow University of Technology, Warszawska 24, 31-155 Kraków, Poland*

---

### Abstract

The results of a series of experimental laboratory and numerical tests of Polymer Flexible Joint (PFJ) under shear load have been presented in this paper. To determine the suitability of technology in practical use in precast concrete pavements it is very important to describe correctly the mechanical behavior of PFJ subjected to shear load. This work presents the results of 24 experimental laboratory tests performed on middle-sized PFJ specimens of various geometry loaded with shear. All specimens have been modeled in Abaqus 6.12. The convergence of data computed and tested has been shown for all variants. The results computed for a real scaled structure with PFJ have been also presented in the paper, providing a basis for further research and aiming at the implementation of this technology.

© 2015 Published by Elsevier Ltd. This is an open access article under the CC BY-NC-ND license

(<http://creativecommons.org/licenses/by-nc-nd/4.0/>).

Peer-review under responsibility of organizing committee of the 7th Scientific-Technical Conference Material Problems in Civil Engineering

**Keywords:** concrete; laboratory; numerical; pavements; polymer flexible joint; shear

---

### 1. Introduction

Shear force is a very important internal force in some types of precast concrete pavements. Shear stress can be dominant in the design of precast concrete slabs, for example in aircraft pavements with high value concentrated loads coming from plane wheels. Shear load can be responsible for slab edge and expansion joint damage occurring in concrete slabs even after a couple of years of exploitation [1].

---

\* Corresponding author. tel.: +48-12-628-23-53.

E-mail address: [pkisiel@pk.edu.pl](mailto:pkisiel@pk.edu.pl)

Polymer Flexible Joint (PFJ) is a technology of structural connection between elements made of traditional building materials. It has been developed in the Cracow University of Technology since 2003. The main idea of the joint is to allow the connected elements to expand and simultaneously to transfer load by connection. The level of stiffness in PFJ can be controlled by material choice and geometry design. It has been proved that PFJ use in precast concrete pavements would highly improve the mechanical behavior of the structure and its durability. The limitation of the relative displacements of the slabs would also significantly improve the impermeability of the joint [2,3,4]. The stiffness and bearing capacity of the connection under shear load should be examined firstly in order to determine the usefulness of the PFJ in wider applications in precast concrete pavements. The aim of this work is to describe selected aspects of the mechanics of connection subjected to shear load. An additional aim is to verify previously developed theoretical material model of the PFJ using the performed tests, which would allow the numerical prediction of the stiffness of PFJ of any geometry in the future.

This work is a continuation of previous research. Laboratory tests of the PFJ elements under shear load have been performed for specimens of cross-section dimension below 80 mm. This research concerns a series of 6 geometrical variants of the PFJ with cross-sectional side dimension varying between 100 and 400 mm. New test data obtaining allows a more comprehensive verification of previous constitutive relations derived for PFJ.

### Nomenclature

A	surface of loaded area
$C_{ij}$ , D	temperature-dependent material parameters
d	thickness of the polymer
E	modulus of elasticity
F	the force on the testing machine
$\gamma$	angle of shear
$\tau$	simplified shear stress

## 2. Research description and methodology

### 2.1. Test procedure

A set of laboratory destructive experimental tests were performed firstly concerning middle-sized specimens of geometry which had not been previously tested. The main objective of the tests was to determine the stiffness and bearing capacity of the specimens. Six numerical models in Abaqus 6.12 were then developed, simulating the experiment scheme as closely as possible. Afterwards, the computed and measured data were compared. The comparison is presented at the same graph for various geometrical variants and strain values. Due to quite high data convergence a numerical simulation of PFJ connecting large-sized elements was performed. As a result, the bearing capacity of a real scale construction was calculated.

### 2.2. Experimental laboratory tests

Within this part 24 pieces of specimens of PFJ were tested. 6 sets of tests, 4 pieces of specimens in each, were performed. All specimens were made of C30/37 concrete and PM type polymer. Modulus of elasticity  $E$  for polymer PM is approximately equal to 5 MPa [5]. All elements were constructed specially for this research purposes. The choice of dimensions of the samples allowed us to examine the influence of thickness, width and height change on joint stiffness and capacity. All specimens consisted of three concrete elements connected by two polymer layers. Two external concrete elements were mounted in the machine without rotation ability, while the internal element was loaded, as shown in Fig. 1. There were prepared and tested specimens in 6 geometric variants, as shown in Tab. 1.

The tests were carried out under laboratory conditions with a constant temperature. The influence of UV radiation, chemical agents and rheology was omitted. The strain ratio for all tests was assumed to 100%/min. A testing machine ZWICK Z100 Zwick/Roell with maximum force of 1000 kN was used in this research. All experiments were destructive and were held until 50% force decrease. Images of performed tests are shown in Fig. 1.



Fig. 1. Scheme and dimensions of tested specimens under shear load (on the left), photograph of specimen after failure (in the middle) and specimen before loading (on the right).

Table 1. Dimensions of tested specimens under shear load.

Specimen label	thickness [mm]	width [mm]	height [mm]
100x100x10	10	100	100
100x100x20	20	100	100
100x100x30	30	100	100
200x100x20	20	200	100
400x100x20	20	400	100
100x200x20	20	100	200

### 2.3. Numerical calculations of middle-sized specimens

Abaqus 6.12 software with Finite Element Method was used for the numerical calculations. Quarters of each specimen were modeled in order to reduce computation time. All boundary conditions were set using contact layer between rigid surfaces and concrete elements. The load was represented by the dislocation of a reference point, related to moveable rigid surface located at the upper surface of the internal concrete element.

There were used eight node 3D brick elements C3D8R type for concrete and C3D8H type for polymer [6]. The total number of elements used in calculation ranges from 27,200 to 300,000. The polymer is modeled by hyperelastic Mooney-Rivlin material described by parameters:  $C_{01} = 470152$  Pa,  $C_{10} = -51766$  Pa,  $D = 0$ . Those parameters were calculated for incompressible material, based on previously performed polymer tests [7,8]. Parameters of concrete according to [9] were applied. Dislocation maps of the sample deformed numerical models in axonometric and in cross-section are presented in Fig. 2.

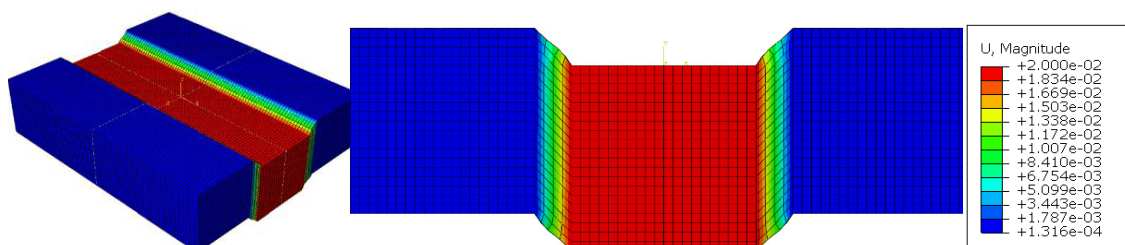


Fig. 2. Dislocation map of numerical model of specimen 400x100x20 in axonometric (on the left) and in cross-section (on the right).

## 2.4. Numerical calculations of a large-sized specimen

Numerical calculations of a real scale specimen were carried out basing on modeling methodology according to description in 2.3. The maximum force in the connection was determined for shear strain values of 25% and 50%. The dimensions and scheme of the modeled element are shown in Fig. 3. In order to reduce computational time, only a quarter of the specimen was modeled. The sample stress map and model visualization is presented in Fig 3.

The results obtained from the simulation are useful in further laboratory tests planning, concerning large-sized elements. This model also shows the value of shear load that may be transferred by PFJ in a practical application.

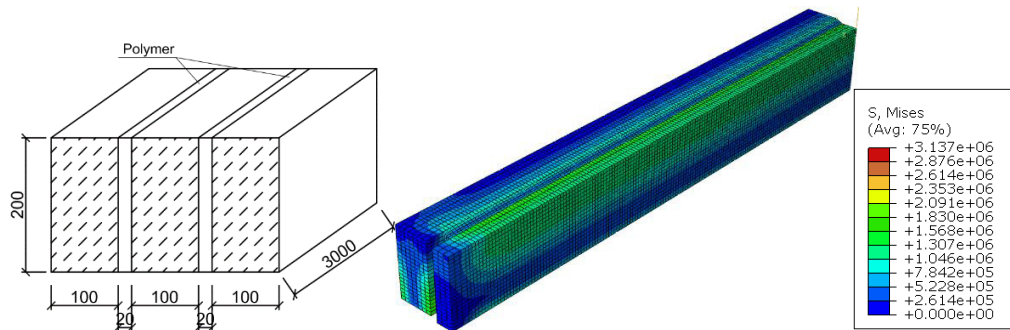


Fig. 3. Scheme and dimensions (on the left) and numerical model visualization with stress map of large-sized element (on the right).

## 3. Results for middle-sized specimens

Fig. 4. presents the results of experimental laboratory tests. An exemplary series of tests of four samples of the same geometrical variant is shown in the force-displacement graph (Fig. 4 a). It can be noticed, that the dispersion of particular specimens is relatively small. The form of destruction is not sudden; shear force after partial damage is still being transferred, which significantly increases the energy of destruction of elements connected by PFJ.

The comparison of stress in tested geometrical variants is shown in Fig. 4 (b), (c). Stress in those graphs is defined as:

$$\tau = \frac{F}{A} \quad (1)$$

while on the horizontal the angle strain is defined as:

$$\gamma = \frac{u}{d} \quad (2)$$

Analyzing the data in full range strain, it can be concluded that stresses do not significantly and clearly depend on a geometrical variant. At a strain range up to 20% the difference in stresses between geometrical variants does not exceed approx. 30%.

The comparison of tested and calculated data is presented in Fig. 5. A rather satisfactory level of convergence for particular specimen sizes can be noted. FEM analysis was run with set of 10 checkpoints for force and displacements. Although at presented scale numerical results may look like a straight line, in fact this data is represented by a function with a small curvature. The biggest difference in the compared data can be noticed for 400x100x20 variant, but the explanation of the different convergence of the presented results is not known yet.

Fig. 6 presents two graphs showing a summary of mean arithmetic values for all geometrical variants obtained in an experimental (on the left) and computational (on the right) manner. The scale and axis range for both graphs is the same. An analysis of the presented graphs may lead to the conclusion that the results converge in both a qualitative and quantitative sense.

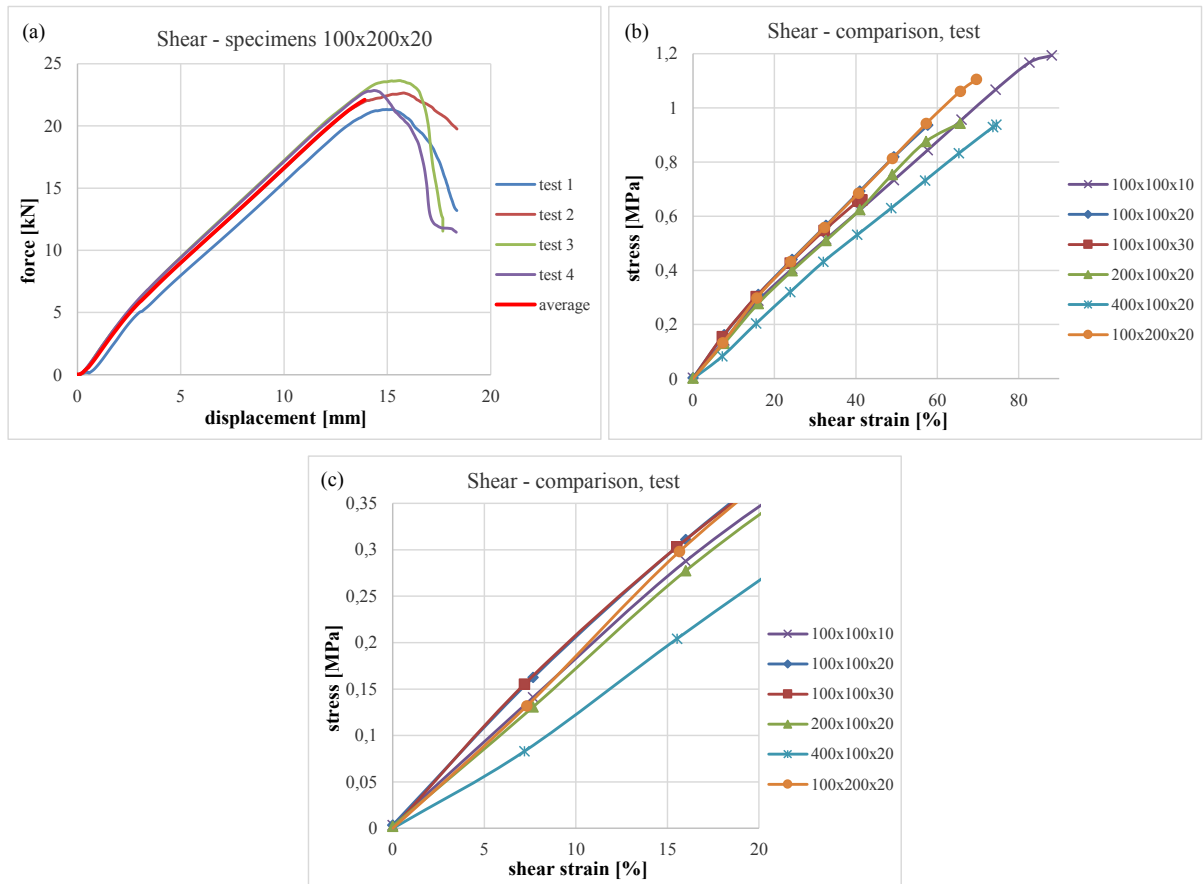


Fig. 4. Results from sample test series for specimens 100x200x20 (a), cumulative result plot of arithmetic means of all test series at full share strain range (b) and at range of 0-20% of shear strain (c).

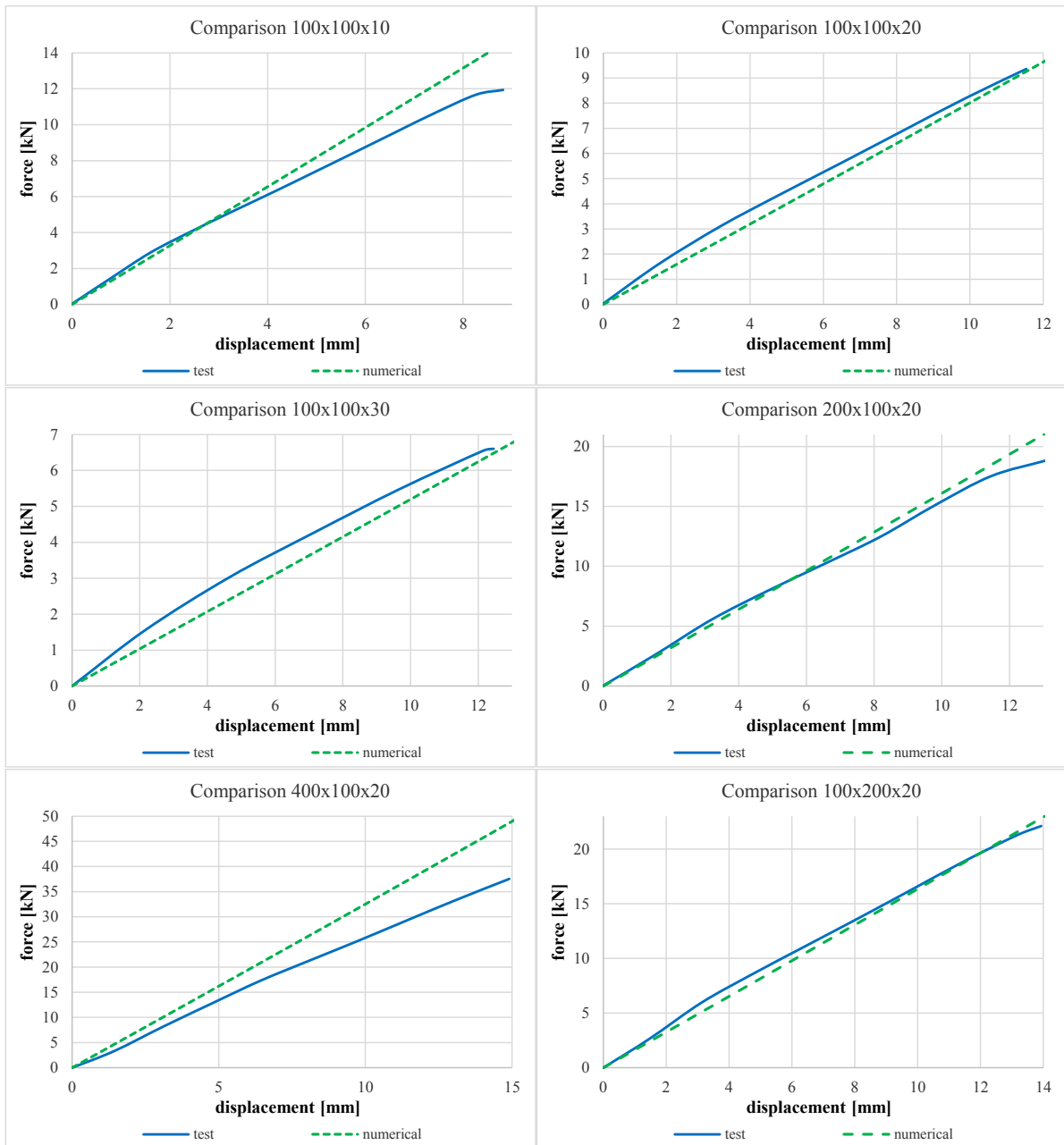


Fig. 5. Comparison of measured and numerically calculated data for all geometrical variants.

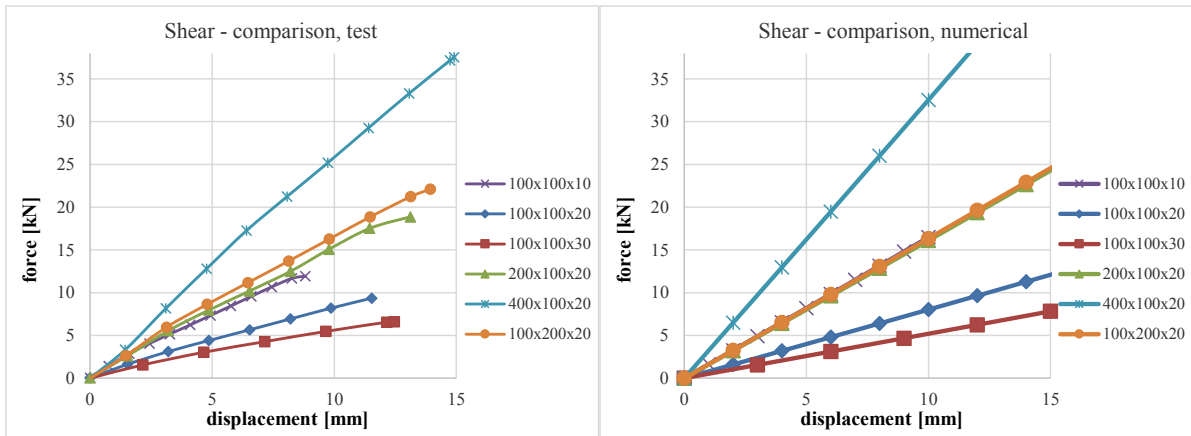


Fig. 6. Cumulative result plot for all test series for experimental laboratory tests (on the left) and for numerical calculations (on the right).

#### 4. Results for large-sized specimen

Calculations of large-sized specimen resulted in maximum force in the PFJ determination. For angle strain of 50% and corresponding displacement of internal concrete element of 1 cm, the calculated force is equal to 512 The resultant value (51.2 t) appears to be relatively high, especially when compared to the values of the live load in concrete pavements. For angle strain of 25%, the calculated force is equal to 128 kN. It is worth noting that the initial modulus of elasticity for polymer PM is equal to approximately 5 MPa, which provides relatively high flexibility of the connection. Confirmation of those values in large-scaled laboratory tests would be very promising for PFJ technology practical application.

Maximum compression stresses in the construction did not exceed 3.2 MPa, as shown in Fig. 7. There is presented a stress map of a cross-section of maximum stress values, located in external concrete element just by polymer layer for both 25% and 50% angle strain. Fig. 7 also presents sample stress maps for both variants in axonometric. It can be concluded, that in such geometry of connection, the stresses are concentrated only at the lower edge of the cross-section. The corresponding stress map with stress concentration at the upper edge of the cross-section can be drawn for internal concrete element. The research concerning the influence of geometry change on stress distribution in the analyzed example might result in valuable knowledge.

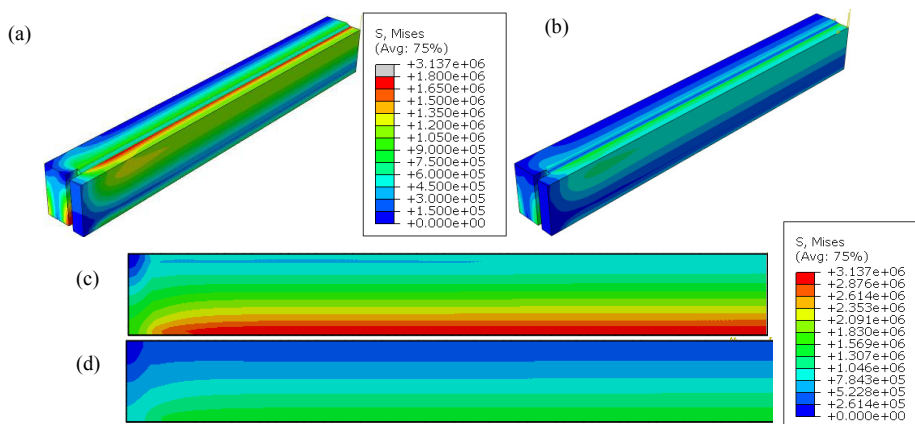


Fig. 7. Mises stress map in the structure in axonometric for 50% strain (a) and 25% strain (b) in the same scale, Mises stress map in cross-section located in concrete next to the polymer layer for 50% strain (c) and 25% strain (d) in the same scale.



## 5. Conclusions

Analyzing the presented results one can conclude that the dependence of change of PFJ connection geometry on stiffness values is not linear. The modeling methodology and material parameters used in numerical modeling provide a relatively high accuracy of calculations and tested data. A comparison of the results does not indicate a big impact of scale effect or testing inaccuracies on the obtained results.

A precise analysis of the presented results can lead to the following conclusions:

- Both experimental and numerical results indicate that the nature of stress-strain characteristics for shear in PFJ connection is close to linear.
- Modeling methodology and material parameters of Mooney-Rivlin form used in this study seem to describe correctly the stiffness of medium-sized PFJ subjected to shear load.
- The bearing capacity of large-sized PFJ elements may be unexpectedly high, for the analyzed cross-section calculated force exceeded 500 kN, this value should be confirmed in laboratory experimental tests.
- The shear load direction in PFJ cross-sections has a very little influence on shear stiffness and bearing capacity. It can be noticed at graphs comparing values obtained for variants 100x200x20 and 200x100x20 and has been proved both experimentally and numerically.
- The damage form of the specimen is not sudden – after partial damage force is still being transferred, which increases the energy of the destruction of samples.
- The maximum deformability of connection without force decrease by 90% has been observed for variant 100x100x10.
- The bearing capacity and maximum deformability increases with the decreasing thickness of the PFJ connection.

Experimental laboratory tests of large-sized specimen will be carried out as a continuation of this research. An examination of the stiffness and bearing capacity of the connection in real scaled structure by *in situ* research is planned.

## Acknowledgements

I am grateful to Arkadiusz Kwiecień Ph.D., D.Sc., Eng. for comments and ACK CYFRONET Krakow for the computer time.

## References

- [1] Kwiecień A., 2010. New repair method of cracked concrete airfield surfaces using of polymer joint, Proc. 13th Int. Congress of Polymers in Concrete - ICPIC 2010 (edit. J.B. Aguiar, S. Jalali, A. Camões, R.M. Ferreira), Funchal - Madeira, Portugal, p. 657-664.
- [2] Delatte N.J., 2014. Concrete Pavement Design, Construction, and Performance. CRC Press.
- [3] Fwa, T.F. (ed.). 2006. Handbook of highway engineering. CRC Press, Taylor & Francis Group.
- [4] Kwiecień A., Gruszczyński M., Zajac B., 2011. Tests of flexible polymer joints repairing of concrete pavements and of polymer modified concretes influenced by high deformations, Trans Tech Publications. Key Engineering Materials Vol. 466 (2011), pp. 225-239.
- [5] Kwiecień A., 2012. Polymer flexible joints in masonry and concrete structures. Monography No. 414, Wydawnictwo Politechniki Krakowskiej, Seria Inżynieria Lądowa, Kraków.
- [6] Abaqus Theory Manual, Abaqus On-line documentation <http://baribal.cyf-kr.edu.pl:2080/v6.7>.
- [7] Kwiecień A., Kuboń P., Zajac B., 2011. Experimental verification of hyperelastic model of polymer on a case study of the flexible polymer joint. Zeszyty Naukowe Politechniki Rzeszowskiej, Rzeszów. (in Polish).
- [8] Nowak, Z., 2007. Constitutive modeling and parameter identification for rubber-like materials. *Engineering Transactions*, vol. 55, No.4.
- [9] EN1992-1-1 Eurocode 2: Design of concrete structures.